Vol. 9: 149–153, 2010
doi: 10.3354/ab00237

AQUATIC BIOLOGY
Aquat Biol

Published online April 27

OPEN ACCESS

Functional morphology of the flounder allows stable and efficient gliding: an integrated analysis of swimming behaviour

Tsutomu Takagi[1,*], Ryo Kawabe[2], Hiroyuki Yoshino[3], Yasuhiko Naito[4]

[1]Faculty of Agriculture, Kinki University, Nara 631-8505, Japan
[2]Institute for East China Sea Research Centre, Nagasaki University, Nagasaki 851-2213, Japan
[3]Hokkaido Industrial Technology Centre, Hakodate 041-0801, Japan
[4]National Institute of Polar Research, Tokyo 173-8515, Japan

ABSTRACT: Although technologies such as archival tags have been developed to monitor the behaviour of free-swimming fish, more advanced techniques are required in order to understand the basis of their behaviour. To assess the glide behaviour of the negatively buoyant Japanese flounder *Paralichthys olivaceus*, we adopted a new approach to examine the importance of the physical aspects of its swimming performance by integrating *in situ* bio-logging data from free-swimming fish with corresponding computational fluid dynamics (CFD) analyses. Field data from the data loggers revealed that flounder commenced powerless glides after swimming upwards. A theoretical simulation of this glide using CFD analysis revealed that the body angle producing the maximum lift/drag ratio was in agreement with the field data and that, during a glide, the moment equilibrium body angle of the flounder resulted in the longest glide distance. This suggests that the morphology of the flounder confers stability on its glide, making this mode of movement more energetically efficient.

KEY WORDS: Flounder · Behaviour · Biomechanics · Morphology · Glide · Bio-logging · CFD · Computational fluid dynamics

Resale or republication not permitted without written consent of the publisher

INTRODUCTION

It is commonly accepted that the morphology of a flatfish lowers its hydrodynamic drag; this is advantageous for a benthic mode of life since it decreases the tendency for a flatfish to be carried downstream by a current while maintaining station on the bottom (Arnold 1969, Arnold & Weihs 1978, Webb 1989). However, flatfish are capable of travelling significant distances in the water column. The plaice *Pleuronectes platessa*, found in the North Sea, can rapidly cover long distances by moving vertically from the seabed into mid-water (Metcalfe et al. 1993, Metcalfe & Arnold 1997). Conventional tagging experiments have shown that Japanese flounder *Paralichthys olivaceus* migrate after release 50 to 100 km during ~1 yr (Tominaga & Watanabe 1998). On the basis of results from a study that used electronic tags, Nashida (1997) hypothesized that the Japanese flounder could increase the distance it travels by repeatedly ascending and descending. In a previous study (Kawabe et al. 2004), we detected both glide and tail-beat swimming modes in free-swimming flounders using data loggers attached to the fish. Weihs (1973) predicted theoretically that fish with negative buoyancy, such as the skipjack tuna and flatfish, could use gliding behaviour to conserve energy. Given the large amplitude of the undulatory motion of the swimming mode in Heterostomata fish such as flounders, a powerless glide following upward swimming markedly enhances energy conservation (Lighthill 1971). Therefore, it appears that flounders may cover long distances by actively coupling glide and tail-beat swimming modes.

Many studies have used electronic tagging to study the behaviour of highly migratory species such as tuna

*Email: tutakagi@nara.kindai.ac.jp

© Inter-Research 2010 · www.int-res.com

and marine mammals (Block et al. 1992, Williams et al. 2000, Davis et al. 2001, Royer et al. 2005). However, we believe that although electronic tagging technology can help us to estimate migration routes, the significance of fine-scale behaviour, such as manoeuvres, cannot be interpreted without a physical understanding of the mechanisms of the movement of fish from a biomechanical perspective. Consequently, analysis of both the kinetic data from electronic tags and the hydrodynamic properties of fish can provide insights that enable us make theoretical predictions regarding kinetics and the efficiency of kinetic energy during movement.

The present study adopted a novel approach that integrates the analysis of field data measured by data loggers attached to free-ranging flounders with computational fluid dynamics (CFD) analyses of flounder movement. Since the latter numerical method can generally estimate the force and the moment acting on the fish body due to the current flow, the direction, speed, and kinetic energy of an individual can be estimated during movement. Therefore, a CFD analysis should be able to contribute to an understanding of the effect of flounder morphology on the ability of the fish to execute fine-scale manoeuvres efficiently and effectively.

In order to assess the swim-and-glide mechanism of the Japanese flounder for energy-efficient movement suitable for long-distance travel, we analysed the hydrodynamic properties of the flounder (such as drag, lift force, and rotational moment) and showed how, in its normal flat position, these properties are rationally designed for gliding.

MATERIALS AND METHODS

Ten flounders *Paralichthys olivaceus* (63.5 ± 3.1 cm total length [TL], 2.54 ± 0.4 kg body weight) were fitted with PD2G data loggers (Little Leonard). These devices measured ambient water temperature, swimming speed, depth, surge acceleration (in the direction of the body axis), and heave acceleration (perpendicular to the body axis). Swimming speed and depth were recorded at 1 s intervals, and heave and surge accelerations at 0.063 and 0.25 s intervals, respectively. In addition, 11 flounder (54.0 ± 4.0 cm TL, 1.55 ± 0.3 kg body weight) were fitted with conventional DT data loggers (Little Leonard) that measured the ambient water temperature and depth only. Depth recordings were conducted at 3 s intervals. More detailed specifications of the data loggers and the procedures for attaching the loggers to the fish are presented in Supplements 1 & 2 (see www.int-res.com/articles/suppl/b009p149_app.pdf).

The fish were released from October to November 2000 in the sea off the south coast of Hokkaido, Japan. Tail beating could be detected from the heave acceleration time-series data recorded by the PD2G loggers. This data, combined with that for the swimming speed and depth, revealed whether an individual was swimming or gliding. The body angle could be estimated from the component of the force of gravitation included in the surge acceleration. Although the DT data loggers were unable to detect the body angle or the tail-beating process, they provided time-series depth data indicating whether a flounder had left the seabed; this data could also be used to estimate the rate of descent. During gliding, the time-series depth data recorded an almost constant rate of descent. The mode of movement was defined as gliding when a flounder sank from over 2 m above the seabed at a nearly constant rate (see Supplements 1 & 2).

CFD analysis allowed us to modify the experimental parameters, such as flow speed and angle of attack (the angle between the longitudinal body axis and the flow direction of a given model). In order to obtain the surface profile of a flounder, we scanned the surface of an individual using a 3-dimensional (3D) non-contact laser surface profiler (VIVID910, Konica Minolta), generating digital data that were decomposed into more than 90 000 polygonal elements. This digitized surface was imported into the CFD programme contained in the SCRYU/Tetra version 7 software package (Software Cradle). The numerical model of the flounder (60 cm TL, 26 cm total height [TH]) was fixed in a rectangular calculation domain of size 3.0 m length × 1.6 m width × 1.6 m height, and the governing equations, the Navier-Stokes and continuity equations, for the fluid inside the domain were solved numerically by the CFD programme using the finite volume method (Rhie & Chow 1983, Ferziger & Peric 1999) (see Supplements 1 & 2).

Assuming that the fluid is incompressible, the Navier-Stokes (Eq. 1) and continuity equations (Eq. 2) can be expressed as follows:

$$\frac{\partial \boldsymbol{U}}{\partial t} + (\boldsymbol{U} \cdot \nabla)\boldsymbol{U} = \boldsymbol{F} - \frac{1}{\rho}\nabla p + \frac{\mu}{\rho}\nabla^2 \boldsymbol{U} \quad (1)$$

$$\nabla \cdot \boldsymbol{U} = 0 \quad (2)$$

where $\boldsymbol{U}$ is the fluid velocity vector, $\boldsymbol{F}$ is the force vector, ρ is the fluid density, p is the pressure, and μ is the coefficient of viscosity.

The pressure and viscosity stress on each element of the body surface of the model can be calculated by numerically solving the governing equation. Thus we obtained the drag (F_D) and lift (F_L) forces by integrating over the entire body surface; the coefficients of drag (C_D) and lift (C_L), which depend on body shape, were then determined using the following equations:

$$C_D = \frac{F_D}{0.5\rho S U^2} \quad (3)$$

$$C_L = \frac{F_L}{0.5\rho S U^2} \quad (4)$$

where U is the flow speed of the steady flow in the domain and S is the surface area of the body.

The glide angle (γ), glide speed (V), and rate of sinking (S_R) can be estimated from the hydrodynamic coefficients under various conditions using CFD analysis as follows (see Supplement 1 & 2):

$$\gamma = \tan^{-1}(C_D / C_L) \quad (5)$$

$$V^2 = W / \left(0.5\rho S \sqrt{C_L^2 + C_D^2}\right) \quad (6)$$

$$S_R = V \sin\gamma \quad (7)$$

where W is the submerged weight. The lift/drag ratio (C_L/C_D) is an important parameter that reflects gliding ability; this ratio changes with changes in the angle of attack. From Eqs. (5) to (7), Eq. (7) can be transformed into the following equation for calculating the non-dimensional rate of sinking, S_R^*:

$$S_R^* = S_R \sqrt{\frac{\rho S}{W}} = \frac{\sqrt{2} C_D}{\left(\sqrt{C_L^2 + C_D^2}\right)^{\frac{3}{2}}} \quad (8)$$

Eq. (8) shows that S_R^* can be determined from measured values but also estimated uniquely from the CFD results using C_D and C_L. Consequently, S_R^* from the field data can be compared with the theoretical value without any size effects.

Values are presented as mean ± SD unless otherwise indicated.

RESULTS

Two flounders (A1 and A2) fitted with PD2G data loggers were retrieved through commercial fishing. The TL and weight of both were ca. 60 cm and 2.2 kg, respectively. The duration of data logging was 1.4 and 5.2 d, respectively. Although the PD2G records showed that the flounders spent more than 90% of the time resting on the seabed, the data also showed that these fish either swam horizontally near the seabed by beating their tails continuously, or they entered a powerless glide without tail-beating following active upward swimming (Fig. 1). While gliding, the mean rate of sinking was 12.8 ± 8.5 and 8.4 ± 2.1 cm s^{-1}, the mean body angle was −5.5 ± 4.9° and −5.8 ± 3.0° (Fig. 2a), and the mean glide speed was 34.1 ± 8.1 and 26.5 ± 7.6 cm s^{-1} for flounders A1 and A2, respectively (Kawabe et al. 2004).

Six individuals fitted with DT data loggers were also retrieved. Their TLs and weights ranged from 50.2 to

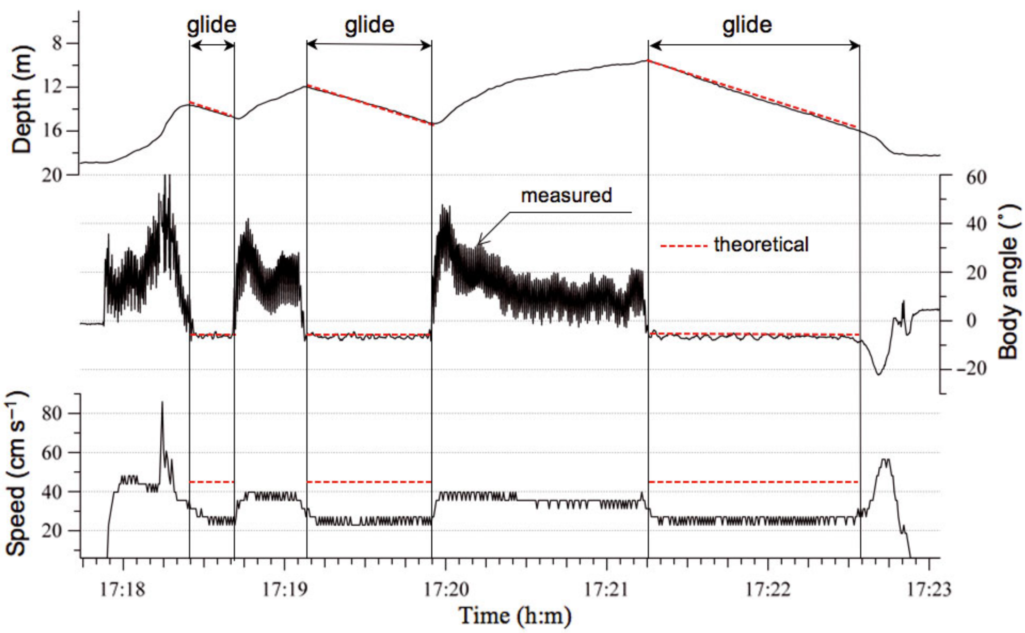

Fig. 1. *Paralichthys olivaceus*. Typical profiles of the swimming depth (sampling rate, 1 Hz), body angle (4 Hz), and swimming speed (2 Hz) for flounder A2 during vertical movement with gliding from the PD2G logger. Dashed lines are values calculated at the maximum lift/drag ratio in the computational fluid dynamics analysis. The body angle was obtained from the component of gravity included in the surge acceleration; negative values indicate a downward angle. Swimming speed was determined from the turbine rotating in the water

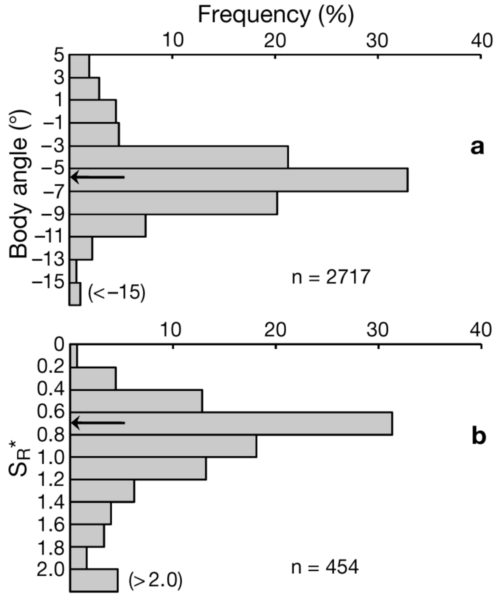

Fig. 2. *Paralichthys olivaceus*. (a) Frequency distribution of body angle determined from the PD2G loggers attached to flounders A1 and A2. The arrow indicates the theoretical value of the body angle using Eq. (5) at the maximum lift/drag ratio. (b) Frequncy distribution of the nondimensional rate of sinking, S_R*, for the DT and PD2G loggers. The arrow indicates the theoretical value of S_R* calculated from Eq. (8) at the maximum lift/drag ratio using computational fluid dynamics analysis. S_R* must be independent of size, since C_D and C_L are nearly constant values in the range of Reynolds numbers 1.0×10^5 to 3.0×10^5

63.4 cm and 1.2 to 2.4 kg, respectively. The duration of data logging was 6.2 to 25.3 d (see Supplements 1 & 2). One individual moved away from the seabed by more than 2 m on only 2 occasions and was therefore not used in the analysis. For the remaining 5 individuals, the mean rate of sinking ranged from 7.7 ± 1.7 to 13.8 ± 5.0 cm s^{-1}. Values of S_R* from the data measured by the PD2G and DT loggers are shown in Fig. 2b and averaged 0.96 ± 0.57 (n = 454); the mode of the distribution was 0.6 to 0.8.

In the CFD analysis, the drag and lift forces acting on the model flounder and the pitching moment of rotation around the centre of gravity in a steady flow were estimated while changing the angle of attack of the longitudinal body axis to the flow direction (Fig. 3).

The cross-section of the surface profile along the longitudinal body axis is similar to that of a cambered aerofoil. Consequently, this allows us to predict qualitatively that a gliding flounder can produce a lift force with its body, the magnitude of which is dependent on the angle of attack, but with less drag force due to the typically low angles of attack. The lift force at an angle of attack of 2° is 5 times greater than the drag (88 and 17 % of the submerged weight, respectively) when the flow speed is 50 cm s^{-1}. When the angle of attack doubles, the lift force is sufficient to lift the body.

Fig. 3 clearly shows the angle of attack at which the flounder exhibits the longest glide distance. The glide distance is maximized at an angle of attack of approximately 4°, when C_L/C_D is greatest. At the maximum C_L/C_D, the rate of sinking, glide speed, and body angle can be estimated using Eqs. (5) to (8) through the CFD analysis; this analysis indicated that flounder A2 could attain a sinking rate of 7.7 cm s^{-1}, a glide speed of 45.0 cm s^{-1}, and a body angle of –5.7°. In Fig. 1, the theoretical values are compared with the field data for flounder A2. The body angle and the rate of sinking were in good agreement with the field data; however, there was a notable difference in the glide speeds.

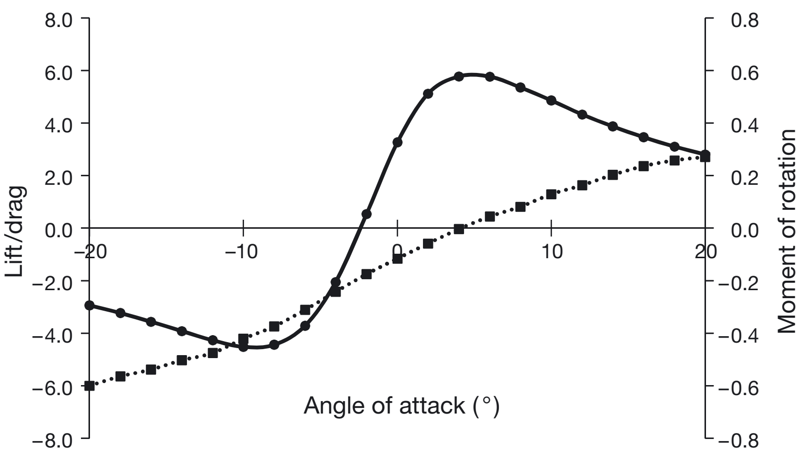

Fig. 3. Lift/drag ratio (solid line) and pitching moment of rotation about the centre of gravity (dashed line) of the models versus the angle of attack during steady gliding calculated in the computational fluid dynamics analysis. The moment of rotation was divided by the mass of the body times the flow velocity squared and is dimensionless

The theoretical value of the body angle for flounders A1 and A2 and S_R* for all tagged flounders, obtained from Eqs. (5) and (8) when C_L/C_D is at a maximum, are –5.7° and 0.69, respectively, and both are in the mode of the histogram of the field data as shown in Fig. 2a, 2b.

Fig. 3 shows that the angle of attack when the moment of rotation was zero occurred at approximately 4° when C_L/C_D was at a maximum.

DISCUSSION

When the theoretical values are compared with the field data, the good agreements for body angle and sinking rate suggest that flounder can glide for long distances with its body flattened (as was the case for flounder A2). However, there was a notable difference in the theoretical and empirical glide speeds. The main reasons for this discrepancy are considered to be the vortex flow present on the ocular side of the fish and the creation of boundary layer gradient effects during the glide; both of these effects can impede accurate measurement of the glide speed. The CFD analysis indeed revealed that a bound vortex flow occurred around the side fin on the ocular side, near to where the logger was mounted (see Supplements 1 & 2).

Although flounders A1 and A2 had similar body weights, in the case of flounder A1 the theoretical rate of sinking was not in close agreement with the field data. It is conceivable that the duration of recording (1.4 d) for flounder A1 was too short to record a sufficient number of gliding episodes; therefore, the non-dimensional rate of S_R^* from the PD2G and DT loggers, which can compare the field data with the theoretical data, excluding the possible size effects, provides confidence in our measurements of the rate of sinking. The large peak in S_R^*, shown in Fig. 2b, supports the interpretation that tagged flounders often glide during descent swimming. Additionally, the theoretical value of S_R^* obtained from Eq. (8) at an angle of attack of 4°, when the lift/drag ratio is at a maximum, is in good agreement with the mode of the histogram (Fig. 2b). This suggests that flounders can glide for long distances during descent mode using features of their morphology.

In order to maintain its body angle for steady gliding, the moment of rotation of the flounder must be almost zero, as any disturbance of this equilibrium will cause rotational motion. We therefore investigated the relationship between the pitching moment of rotation around the centre of gravity and the angle of attack in the CFD analysis (Fig. 3). Interestingly, the coincidence of the angle of attack when the cross point of the moment of rotation was zero and the lift/drag ratio was at a maximum suggests that the equilibrium body angle with respect to the angular moment results in the longest glide distance when the flounder adopts its normal flat posture. This means that a gliding flounder exhibits both stability and efficient movement, and also supports the hypothesis that for fish with negative buoyancy, such as flatfish, a powerless glide followed by active upward swimming is energetically more efficient for traversing a given horizontal distance than continuous swimming, as pointed out by Weihs (1973). The integrated analysis of CFD and bio-logging data will help us in future studies to elucidate the significance of the physical aspects of aquatic animal behaviour.

Acknowledgements. We thank Drs. D. Weihs and R. W. Davis for their helpful comments. We also thank Dr. T. Hiraishi for his assistance with the CFD application.

LITERATURE CITED

Arnold GP (1969) The reactions of the plaice (*Pleuronectes platessa* L.) to water currents. J Exp Biol 51:681–697

Arnold GP, Weihs D (1978) The hydrodynamics of rheotaxis in the plaice (*Pleuronectes platessa* L.). J Exp Biol 75: 147–169

Block BA, Booth D, Carey FG (1992) Direct measurement of swimming speeds and depth of blue marlin. J Exp Biol 166:267–284

Davis RW, Fuiman LA, Williams TM, Le Boeuf BJ (2001) Three-dimensional movements and swimming activity of a northern elephant seal. Comp Biochem Physiol A 129: 759–770

Ferziger JH, Peric M (1999) Computational methods for fluid dynamics. Springer, Berlin

Kawabe R, Naito Y, Sato K, Miyashita K, Yamashita N (2004) Direct measurement of the swimming speed, tailbeat, and body angle of Japanese flounder (*Paralichthys olivaceus*). ICES J Mar Sci 61:1080–1087

Lighthill MJ (1971) Large-amplitude elongated-body theory of fish locomotion. Proc R Soc Lond B 179:125–138

Metcalfe JD, Arnold GP (1997) Tracking fish with electronic tags. Nature 387:665–666

Metcalfe JD, Holford BH, Arnold GP (1993) Orientation of plaice (*Pleuronectes platessa*) in the open sea: evidence for the use of external directional clues. Mar Biol 117:559–566

Nashida K (1997) Behaviour analysis of Japanese flounder by using micro data-logger. Gekkan Kaiyo 29:149–153 (in Japanese)

Rhie CM, Chow WL (1983) Numerical study of the turbulent flow past an airfoil with trailing edge separation. AIAA J 21:1525–1532

Royer F, Fromentin JM, Gaspar P (2005) A state-space model to derive bluefin tuna movement and habitat from archival tags. Oikos 109:473–484

Tominaga O, Watanabe Y (1998) Geographical dispersal and optimum release size of hatchery-reared Japanese flounder *Paralichthys olivaceus* released in Ishikari Bay, Hokkaido, Japan. J Sea Res 40:73–81

Webb PW (1989) Station-holding by three species of benthic fishes. J Exp Biol 145:303–320

Weihs D (1973) Mechanically efficient swimming techniques for fish with negative buoyancy. J Mar Res 31:194–209

Williams TM, Davis RW, Fuiman LA, Francis J and others (2000) Sink or swim: strategies for cost-efficient diving by marine mammals. Science 288:133–136

Editorial responsibility: Söhnke Johnsen, Durham, North Carolina, USA

Submitted: May 15, 2009; Accepted: February 10, 2010
Proofs received from author(s): April 16, 2010